Pattern selection in multi-layer network with adaptive coupling

Peihua Feng
Xi'an Jiaotong University
Ying Wu (wying36@163.com)
School of Aerospace Engineering, Xi'an Jiaotong University https://orcid.org/0000-0002-1298-3038

Research Article

Keywords: Chimera state, Multi-layer network, Adaptive coupling

Posted Date: May 13th, 2021

DOI: https://doi.org/10.21203/rs.3.rs-497918/v1

Noname manuscript No.
(will be inserted by the editor)

Pattern selection in multi-layer network with adaptive coupling

Peihua Feng · Ying Wu

Received: date / Accepted: date

Abstract Feed-forward effect modulates collective behavior of a multiple neuron network and facilitates strongly synchronization of their firing in deep layers. However, full synchronization of neuron system corresponds to functional disorder. In this work, we investigate coexistence of synchronized and incoherent neurons in deeper layer (called chimera state) in order to avoid the contradiction between facilitation of full synchronization and complete functional failure of neuron system. We focus on a multiple network containing two layers and confirm that chimera state in layer 1 could also induce that in layer 2 when the feed-forward effect is strong enough. Cluster also is discovered as a transient state which separates full synchronization and chimera state and occupy a narrow region. Both feed-forward and back-forward effect together emerge of chimera states in both layer 1 and 2 under same parameter in large range of parameters selection. Further, we introduce adaptive dynamics into inter-layer rather than intra-layer couplings. Under this circumstance chimera state still can be induced and coupling matrix will be self-organized under suitable phase parameter to guarantee chimera formation. Indeed, chimera states exist and transit to deeper layer in a regular multiple network with very strict parameter selection. The results helps understanding better the neuron firing propagating and encoding scheme in a multi-layer neuron network.

Keywords Chimera state · Multi-layer network · Adaptive coupling

Peihua Feng
State Key Laboratory for Strength and Vibration of Mechanical Structures, School of Aerospace Engineering, Xi'an Jiaotong University, Xi'an 710049, P.R.China
Tel.: +010-18092561257
Fax: +123-45-678910
E-mail: fphd2017@xjtu.edu.cn

Ying Wu
State Key Laboratory for Strength and Vibration of Mechanical Structures, School of Aerospace Engineering, Xi'an Jiaotong University, Xi'an 710049, P.R.China
E-mail: Wying36@xjtu.edu.cn

1 Introduction

Information propagates from one functional group of neurons to another to facilitate cooperation of different brain regions, providing fundamental function of cognitive ability[1]. More important, many evidences show that nervous system in cortex exhibits a multi-layer structure[2]. It is also usually believed that the brain networks are considered as fundamental multi-entities with diverse scales[3]. Richard F. B. et al. further understand the definition of multi-scales network in space, time and topology respectively according to the context[4]. Sarah F. M. et al. propose that a principled framework of multi-layer network allows one to develop network statistics to combine different aspects including structure and function of brain[5]. Links between layers reflect interactions between aspects. In summary, considering the various entities of brain network and their collaborative work to achieve diversity of complex brain functions, a neuronal network with multi-layer structure is a reasonable model to investigate collective dynamics and interactions between different groups of neurons.

Rich dynamics have been studied in the multi-layer neuronal network due to its wide range of applications in complex systems from various disciplines[6–8]. Generally speaking, adding connections or increasing coupling strength usually facilitate synchronization among the oscillators inter- and intra-layer according to previous studies on stability analysis on multi-layer network[9–11]. One-way interactions between inter-layers called feed-forward effect, even when the couplings distribute randomly among neurons locating the adjacent layers, is proved to have a great ability to facilitate synchronization of neurons firing[12]. However, as a matter of fact, synchronization in large scale of neuron firing usually relates to epilepsy, a typical brain functional disorder state[13–15]. The fact that all neurons fire in a complete same rhythm indicates they loss their abilities of coding and decoding. Therefore, partial synchronization enters our field of vision due to its possibility of balance between synchronization in neurons' collective behaviors and demand for information processing in the nervous system with a multi-layer structure.

A counterintuitive phenomenon called chimera is the exact partial synchronization which allows that synchronized oscillators and disordered oscillators coexist stably in a network. It is first discovered by Kuramoto and his colleagues in Ginzburg-Landau equations with nonlocal coupling[16–18]. Then it is named after a strange creature in Greek mythology, whose different parts come from different animals, indicating a coexistence of different type of states[19]. In the past two decades, chimera states are discovered and well studied in a large variety of systems from phase coupled systems[20, 21] to neuronal network[22] or time-discrete coupled map system[23] and from regular networks[24–26] to complex networks[27–29]. Researches on chimera states do not restrict to depicting its existence and properties[30]. As to its application, scholars try understand the work principle of brain in the framework of chimera state and gain further insight into spatiotemporal patterns of regional brain activity. Unihemispheric sleep observed in animals[31] and human beings' brain[32], in which left and right hemispheres synchronize in different

levels, is usually considered as a typical chimera state. Further, relationships between chimera and epileptic seizures are discovered[33,34] and they allow us to alert epilepsy two hours in advance by calculating Kuramoto order parameter[35].

In our study, we focus on chimera states in multiplex neuron network to explore the possibility of partially of keeping coding and decoding ability in multiple network with feed-forward effect. As a matter of fact, the problem has already aroused interests of scholars. Ghosh and his colleagues investigate birth and death of chimera states in a double layer network described by time-delay chaotic maps and they find their existence is sensitive to time-delay of coupling inter-layers[36]. Then they replace time-discrete oscillators by Hindmarsh-Rose neurons linked by electrical synapses intra-layers and chemical synapses inter-layers, and observe quorum sensing mechanism for the chimera formation[37, 38]. Yang et. al. discover chimera states and their rich dynamics in a bipartite network in which neurons do not couple with each other when they locate in same layers[39]. In addition, considering the flexibility of brain network, our study also takes spike-timing-dependent plasticity (STDP) into account[40–42]. The brain is always reshaping its topology especially the connection weights. Liu et. al. numerically prove the existence of chimera state in complex network and a realistic network of cerebral cortex with adaptive coupling[43].

Materials are list as follows, neuron model and structure of multi-layer network with feed-forward and feed-forward effect are introduced in Section. 2. Pattern selection in multi-layer network and formation process of chimera state are studied in Section. 3. In Section 4, we investigate pattern formation for both layer 1 and 2 with considering both feed-forward and feed-backward effect and their corresponding selections. Spike-timing dependent plasticity is introduced into intra-layer couplings in Section 5, and we explore the conditions of existence of chimera states. Finally, we draw our conclusions and prospects in Section. 6.

2 Model of neuron and multi-layer neuronal network.

The multi-layer neuronal network in our study consists of 2 layers of neurons arranged in a ring topology with $N = 256$ neurons for each layer. The coupling for every neuron comes from two parts. One of them is interaction among $2R$ adjacent neurons locating the both sides of it symmetrically in the same layer (intra-layer) and another one is coupling from $2R$ corresponding neurons in the other layer (inter-layer). The feed-forward effect is achieved by the fact that the neurons in the second layer are coupled with those in the first layer. In our study, the multi-layer neuronal network is described by a system of FitzHugh-Nagumo (FHN) neurons with interactions,

For the neurons in the first layer:

$$\begin{aligned}
\varepsilon\dot{u}_{i,1} =& u_{i,1} - \frac{u_{i,1}^3}{3} - v_{i,1} + \frac{c_1(1-r_1)}{2R}\sum_{h=i-R}^{h=i+R}[u_{h,1}(t-\tau_1) - u_{i,1}] \\
&+ \frac{c_1 r_1}{2R}\sum_{h=i-R}^{h=i+R}(1+\lambda_{h,i}^1)[u_{h,2}(t-\tau_2) - u_{i,1}] \qquad (1)\\
\dot{v}_{i,1} =& u_{i,1} + a \\
\dot{\lambda}_{h,i}^1 =& -\gamma[\sin(u_{h,2}(t-\tau_2) - u_{i,1} + \beta) + \lambda_{h,i}^1]
\end{aligned}$$

For the neurons locating in the second layer:

$$\begin{aligned}
\varepsilon\dot{u}_{i,2} =& u_{i,2} - \frac{u_{i,2}^3}{3} - v_{i,2} + \frac{c_2(1-r_2)}{2R}\sum_{h=i-R}^{h=i+R}[u_{h,2}(t-\tau_3) - u_{i,2}] \\
&+ \frac{c_2 r_2}{2R}\sum_{h=i-R}^{h=i+R}(1+\lambda_{h,i}^2)[u_{h,1}(t-\tau_4) - u_{i,2}] \qquad (2)\\
\dot{v}_{i,2} =& u_{i,2} + a \\
\dot{\lambda}_{h,i}^2 =& -\gamma[\sin(u_{h,1}(t-\tau_4) - u_{i,2} + \beta) + \lambda_{h,i}^2]
\end{aligned}$$

where $i = 1, 2, \cdots, N$. Subscripts for membrane potential u and slow variable v denote index of neurons inside layer and the layer number respectively. $\varepsilon = 0.05$ in our study is scale parameter. For ith neuron, $2R$ is the number of neurons in the same layer and the other layer coupling with it and they distribute symmetrically in its neighbor. c_1 and c_2 are coupling strength for neurons in the first and second layer. $\tau_{1,2,3,4}$ are time delays in coupling intra-layer and inter-layer for the layer 1 and 2. $r_1, r_2 \in (0,1)$ and $(1-r_1), (1-r_2)$ describe ratios of coupling inter-layer and inter-layer for neurons in layer 1 and 2 respectively. In particular, r_1 and r_2 are magnitudes of the feed-forward effect and feed-back effect, and they measure the competition between coupling of inter-layer and of intar-layer.

We introduce time-dependent λ_{ij} to represent adaptive coupling between neurons. The previous study already proves that chimera state can survive in a single layer of complex network with coupling network. In our study, we focus interactions across layers, therefore intra-layer coupling is predetermined and fixed but inter-layer interaction is governed by a series of first order ordinary differential equations and mainly controlled by the phase difference of the coupled neurons. γ is a small parameter and set as 0.01. β is a key parameter determining the coupling mode. $\beta \approx -\pi/2$ means Hebbian-like rule because the coupling strength increases for a pair of in-phase neurons and decreases for a pair of anti-phase neurons. $\beta \approx \pi/2$ in contrary denote anti-Hebbian-like rule. β around 0 indicates asymmetric Hebbian rule.

The structure of multi-layer neuronal network is illustrated by Fig. 1. It composes 2 layers in the network, and each of them contains $N = 256$ neurons

illustrated by blue circles. Black lines with arrows denote coupling among neurons inside the layer and red lines with arrows represent coupling from the upper layer which is considered as the feed-forward effect. Feed-backward effect is illustrated by green arrow lines. Runge-Kutta algorithm is employed to solve the equations and time step is chosen as 0.01ms.

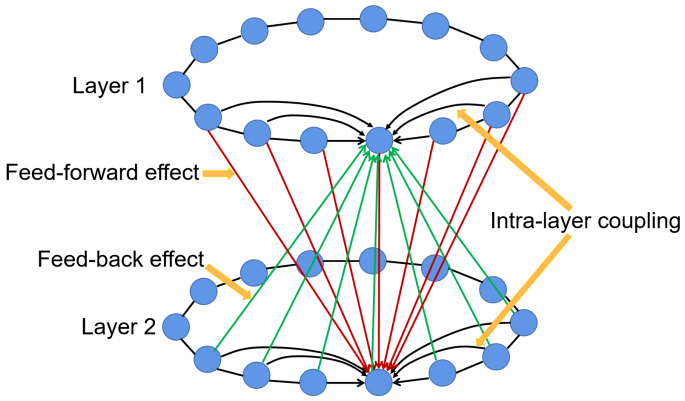

Fig. 1: Multi-layer structure of neuronal network.

3 Chimera state in multi-layer network

In this section, we investigate the existence of chimera state of layer 2 induced by emergence of it in the first layer. Therefor, only the feed-forward effect rather than feed-backward coupling is kept in this section, namely, $r_1 = 0$. First, in order to generate chimera we choose carefully the initial condition that u and v distribute evenly randomly in a circle $u_i^2 + v_i^2 = 4$ for the layer 1. The mean phase velocity $< \omega_i >$ is the key parameter to distinguish disordered and synchronized oscillator. Discontinuous $< \omega_i >$ embedded in continuous $< \omega_i >$ means the unsynchronized oscillators burst out of synchronized oscillators, which indicates a scenario of a chimera state.

We first show the chimera state in the layer 1 with mean phase velocity $< \omega_i >$ considered (Fig. 2), and it is calculated by

$$< \omega_{i,j} >= \frac{2\pi M_{i,j}}{\Delta T} \tag{3}$$

where $M_{i,j}$ denotes the neuron firing number of ith neuron in jth layer if its $u_{i,j}$ is beyond a threshold value $u_{th} = 0$mV during the time span $T = 1000$s. Electrical activity of a neuron is considered as oscillator's behavior. A single neuron firing is equivalent to phase change of oscillator by 2π. The index of

mean phase velocity distinguishes the synchronized oscillators and disordered ones by distribution of values of it in parameter space. Synchronized oscillators take same values of mean phase velocity $< \omega_i >$ and different values of it for the disordered oscillators. Snapshots of membrane potential u and slow variable v at $T = 10000$ms are shown in Fig. 2(a) and (c). The values of them are divided by continuous distribution and random distribution representing synchronized oscillators and unsynchronized oscillators. Chimera state is also represented much more clearly by a spatial-temporal pattern illustrated by Fig. 2(b), in which continuous distribution for u for synchronized neurons are separated by disordered neuron regions. The mean phase velocity is calculated during the interval of 9000ms$< T <$ 10000ms, and they distribute corresponding to whether they are synchronized (Fig. 2(d)).

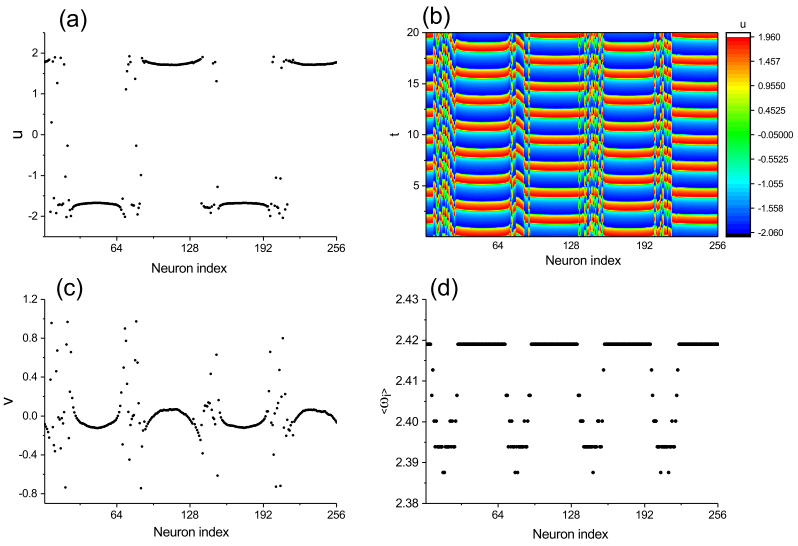

Fig. 2: Chimera state in the first layer of multi-layer network.(a) Distribution of u at $T = 10000$ms, (b) Spatial-temporal pattern during 9980ms$< T <$10000ms, (c) Distribution of v at $T = 10000$ms, (d) Distribution of $< \omega_i >$ during 9000ms$< T <$10000ms

Initial values of neurons are set as zeros for the layer 2. We do not consider spike-timing dependent plasticity in this section and set all the weight of links as steady states by $\lambda^2_{i,j} = 1$ for all the neurons. For simplicity time delay of feed-forward effect is chosen the same as those for intra-layer coupling, $\tau_1 = \tau_3 = \tau_4 = 1.0$. r_2 denotes ratio of feed-forward effect (inter-layer) compared to intra-layer coupling and can be considered as a key parameter. We illustrate

snapshots of membrane potential of neurons in layer 2 as well as their $< \omega_i >$ in Fig. 3.

There exists a critical value of $r_{1cr} = 0.344$ only beyond which does chimera state emerge in layer 2. Membrane potentials of neurons distribute in a continuous curve and all their mean phase velocities keep the same and unchanged when $r_1 < r_{1cr}$ (first and second rows in Fig. 3). Neuron firings oscillate in a harmonic form with small fluctuations in the peaks when $r_1 = 0.1$. But neurons split into eight parts, distributing alternatively along the neuron indexes. Four of them represent continuous distribution of membrane potential and complete the same value of $< \omega_{i,2} >$, but in other four parts membrane potentials distribute randomly, and their $< \omega_{i,2} >$ distribute in multi stair-like structures.

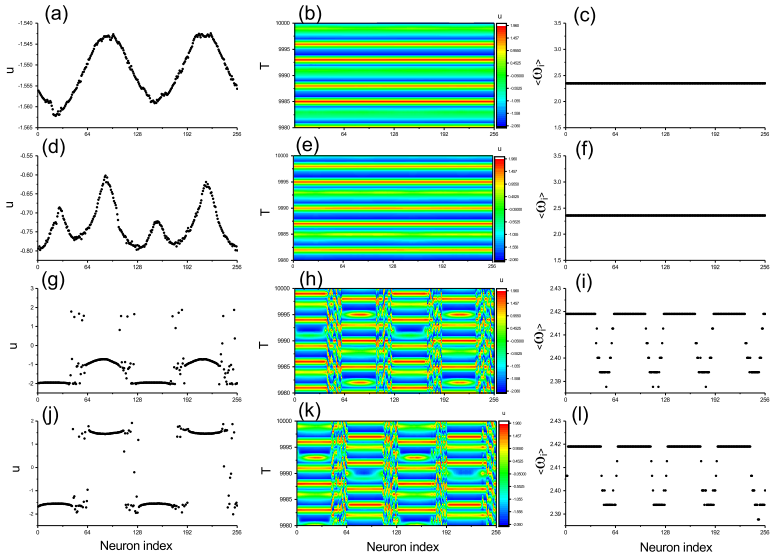

Fig. 3: Pattern formation of layer 2 with different feed-forward effects r_1.(a),(d),(g) and (j) are snapshots for membrane potential with $r_1 = 0.1, 0.3, 0.4$ and 0.9 respectively. (b),(d),(h) and (k) are their corresponding spatial-temporal patterns during 9980ms$< T <$10000ms. (c),(f),(i) and (l) are for the mean phase velocities $< \omega_{i,2} >$ of layer 2 during the last 1000ms

We provide a scenario when $r_2 = 0.356$ which is greater than the critical value a little, to delineate the pattern formation of chimera state. Chimera state emergences for layer 1 and layer 2 during the time span 0ms$< T <$ 3000ms are compared Fig. 4. For layer 1, chimera state emerges after a period of self-organization and generates rapidly at about 300ms with only time-delay intra-layer coupling. However, scenario for layer 2 is more complicate than that for layer 1. Roughly speaking, before birth of chimera state in layer 2, spatial-

temporal pattern formation undergos three stages. First stage last about from zero ms to 1300ms, during which all the neurons firing are synchronized. There is no different for phase velocities of neuron firing. Phase slides appear gradually at the end of this stage, leading that cluster (membrane potentials split into 4 continuous parts and there is no disordered neurons) dominate the layer 2. During the second stage of 1300ms$< T <$ 2100ms, disordered neurons generate from the phase slides. But after a short period of time for competition, domains for synchronized neurons and disordered neurons distribute relatively randomly. The third stage of 2100ms$< T <$ 2400ms is called the transition stage because the domains of disordered neurons degenerate to phase slides. And clusters dominate the spatial-temporal pattern. After the transition stage, disordered neurons are born from the discontinuities of membrane potentials to induce the chimera state when $T >$ 2400ms. Scenario of pattern formation containing three stages for layer 2 can also observed under other strength of feed-forward effect r_2 greater than the critical value.

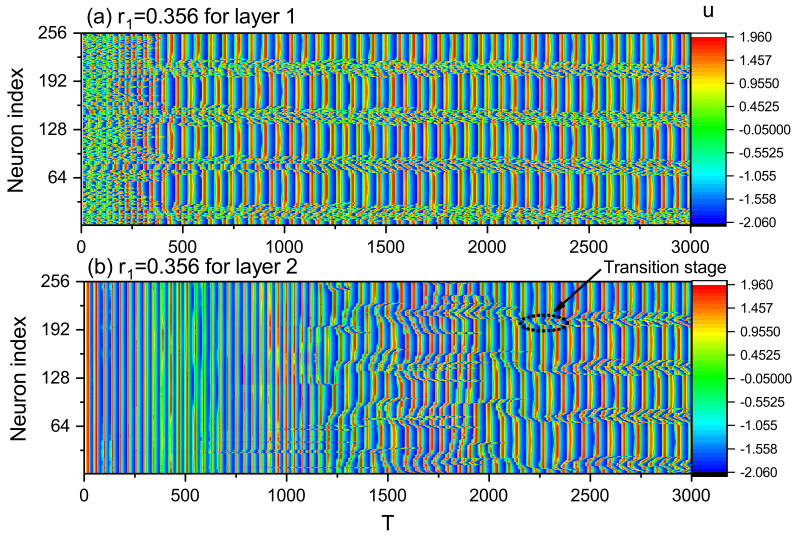

Fig. 4: Comparison of chimera state formation for layer 1 and layer 2 under $r_1 = 0.356$. (a) chimera state in layer 1, (b) chimera formation for layer 2.

In previous study we set all the time-delay as the same value. However, time delay of information propagation depends on their distance. We do not change τ_1 to guarantee the existence of chimera state in the first layer, but investigate chimera formation for a different time delay of τ_4 of inter-layer coupling and τ_3 of intra-layer coupling for layer 2. First, we set time delay for intra-layer coupling for both layer 1 and 2 as the same $\tau_1 = \tau_3 = 1.0$ms and consider τ_4 and r_2 as the parameters. Sweeping the τ_4 and r_1 leads to discovery

of patterns of clusters in very narrow parameter intervals between synchronization and chimera states, denoted by blue area in Fig. 5. Synchronization and chimera state are illustrated by black and gray regions. Clusters demarcate synchronization and chimera state in the parameter space. Scenario of cluster formation is demonstrated in Fig. 7(a)-(c). During its formation process (Fig. 7(c)), all the disordered neurons do not maintain themselves to induce chimera states, instead, they shrink to six isolated discontinuous points which demarcate six continuous membrane potential curves. In other words, spatial-temporal pattern of clusters is discovered in the network. Neurons' mean phase velocities are the same except several points with small discrepancy. Observation during a large span of time tells that the clusters are drifting slowly to the left side with time increasing.

Second, we keep $\tau_1 = \tau_4 = 1$ms fixed and consider τ_3 and r_2 as the parameters to investigate pattern formation when there exists time-delay discrepancy between different groups of neurons. Beside cluster, we also discover a narrow region in double parameter space for a new type of chimera state denoted green area in Fig. 6. Its scenario is shown in Fig. 7(d)-(f). The snapshot represents a chimera state with 2 heads (two continuous domains for synchronized and disordered neurons respectively instead of four of them). The formation process is relatively simple. Disordered neurons burst out of the synchronized ones directly without transition stages (see Fig. 7(f)). Drifting phenomenon can not be observed in chimera state. In other words, once they appear in the network, the domains of disordered and synchronized neurons keep unchanged.

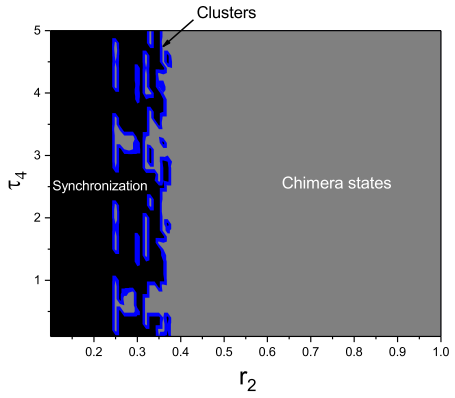

Fig. 5: Distribution of different types of spatial-temporal patterns in layer 2 in double parameter space of τ_4-r_2 plane.

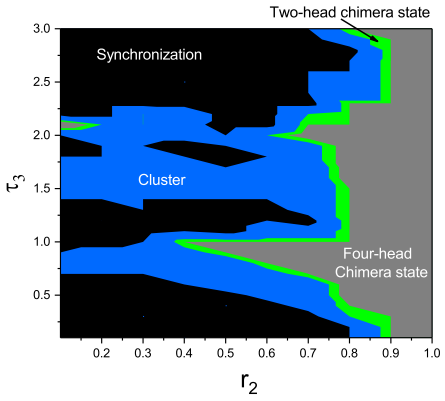

Fig. 6: Distribution of different types of spatial-temporal patterns in layer 2 in double parameter space of τ_3-r_2 plane.

4 chimera formation with both feed forward and backward effect

Beside feed-forward effect, back-forward effect is also considered in this section on pattern formation under bi-directional modification of collective behaviors of both layers. Strength of back-forward r_1 is no longer to set as zero, but a positive value to measure it compared to coupling strength among neurons in layer 1. We consider three cases to demonstrate chimera formation under weak, moderate and strong feed-forward effect. For simplicity we set all the time delay as the same value $\tau_1 = \tau_2 = \tau_3 = \tau_4 = 1$ms. The parameters r_1, r_2 measure the weights of intra-layer coupling compared to inter-layer coupling for every layer. Transition from synchronization to chimera states with weak feed-backward effect is similar to that when there is only feed-forward effect. We take $r_2 = 0.1$ for example (see Fig. 8) and provide snapshots as r_1 increases from 0.1 to 0.4 for layer 1 and 2 at $t = 10000$ms. Patterns are chimera states for both layer 1 and 2 when $r_2 > 0.4$ which are not shown here. Chimera can sustain in layer 1 within the entire span of parameter $0 < r_1 < 1$ (see Fig. 8(a)-(d)). However, in layer 2 there exists a transition from synchronization to chimera state with the critical value of feed-backward effect strength $0.2 < r_{1cr} < 0.3$. Weak feed-forward effect is highly unlikely to facilitate the chimera state in layer 2 unless it combines with feed-backward effect with the strength greater than the critical value.

With strong feed-forward effect ($r_2 = 0.9$), transitions from chimera states to synchronization as increasing r_1 occur for both layer 1 and 2 respectively. We provide snapshots of spatial-temporal pattern under $r_1 = 0.4, 0.5, 0.6$ and 0.7 for layer 1 and 2 in Fig. 9. Patterns of layer 1 and 2 transit from chimera state to synchronization as increasing r_1. Patterns in both layers as r_1 is less than 0.4 and greater than 0.7 are chimera states and synchronized states. Critical values for the transitions are very close.

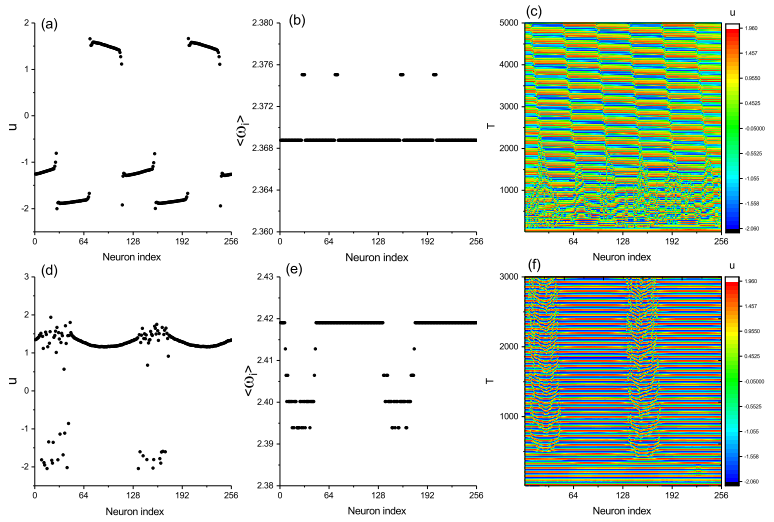

Fig. 7: Spatial-temporal pattern of cluster and chimera with 2 heads. (a), (b) and (c) are snapshots of membrane potential, mean phase velocity $< \omega_i >$ and pattern formation process cluster with $\tau_4 =$ (d), (e) and (f) are scenario of pattern formation for τ.

Chimera states can sustain in second layer for the entire parameter interval $0 < r_1 < 1$ but only survive in partial interval $0 < r_1 < 0.6$ in first layer when a moderate feed-forward effect dominate the coupling among neurons in second layer. Spatial-temporal patterns are listed in Fig. 10 for $r_2 = 0.5, 0.6, 0.7$ and 0.8 when $r_1 = 0.5$. Transition of layer 1 occurs at the critical value $(0.6 < r_1 < 0.7)$ and at the same time patterns become 2 head chimera state from 4 head chimera state. It seems that disordered firing in chimera state is interrupted by synchronized firing. Neurons locating the disordered domains alternate between regular and irregular firings.

We plot distribution of the three typical patterns in the double parameter space ($r_1 - r_2$ plane) for both layer 1 (Fig. 11(a)) and layer 2 (Fig. 11(b). Synchronization, denoted by black region, exists mainly when strength of feed-forward effect r_2 and feed-back effect strength r_1 are large enough and some sporadic areas when r_2 is small. Chimera states (gray regions) occupied the most of the remaining areas. Clusters as the transit pattern illustrated by blue domain, locate in a narrow space between synchronization and chimera states. The distributions for layer 1 and layer 2 can basically overlap, which means that pattern selection for parameters in both layer 1 and 2 is roughly the same when feed-forward and feed-back coupling dominate the multi-layer network at the same time.

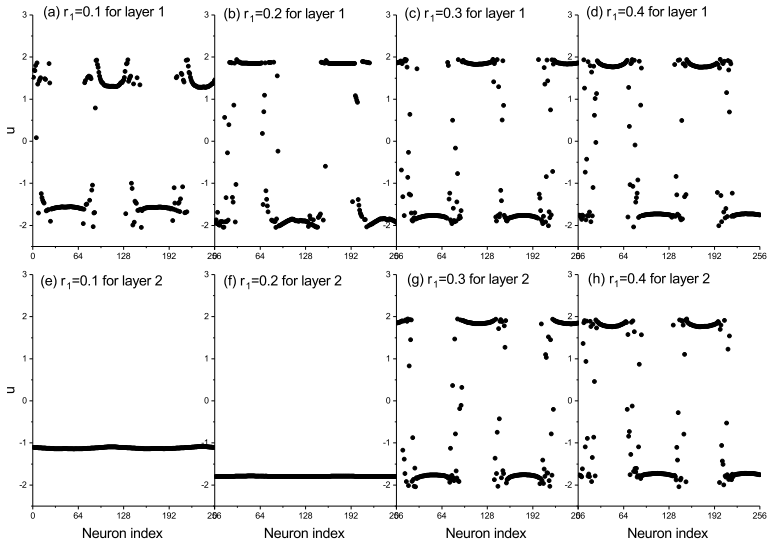

Fig. 8: Snapshots of membrane potentials of neurons in layer 1 (first row) and layer 2 (second row) at 10000ms with small feed-forward effect ($r_2 = 0.1$). (a)-(d) and (e)-(h) are under different feed-back effect strength $r_1 = 0.1, 0.2, 0.3$ and 0.4 respectively.

5 chimera formation under STDP

In this section, we introduce STDP only in inter-layer coupling (feed-forward effect) rather than intra-layer coupling. Feed-backward effect is also neglected, $r_1 = 0$. Time delays for intra-layer coupling for both layers are set as the same value as previous sections, $\tau_1 = \tau_3 = 1.0$ms. Feed-forward effect is chosen as the moderate intensity $r_2 = 0.5$. Coupling cross layers is composed by intra-layer couplings with a constant strength and adaptive coupling from ith neuron in layer 1 to jth neuron in layer 2 whose amplitude is denoted by $\lambda_{i,j}$. Initial values of $\lambda_{i,j}$ is given within $-1 < \lambda_{i,j} < 1$ with uniform distribution. A small constant $\gamma = 0.01$ guarantees that STDP effect is small compered to invariant feed-forward effect and keep the intra-layer couplings fluctuation within a small interval.

Discussion about chimera state in layer 1 is neglected because chimera appears quickly from the beginning. Layer 2 is rich of pattern formation due to parameter selection. We mainly focus on phase lag β because the parameter determines the STDP type: $\beta \to -\pi/2$ means Hebbian-like rule, $\beta \to \pi/2$ indicates anti-Hebbian-like rule and $\beta \to 0$ represents temporally asymmetric Hebbian rule. We provide evolution of spatial-temporal patterns as well as distributions of adaptive coupling strength. Chimera state bursts out of chaotic-like stage at 600ms. Then domains of disordered neurons fluctuates

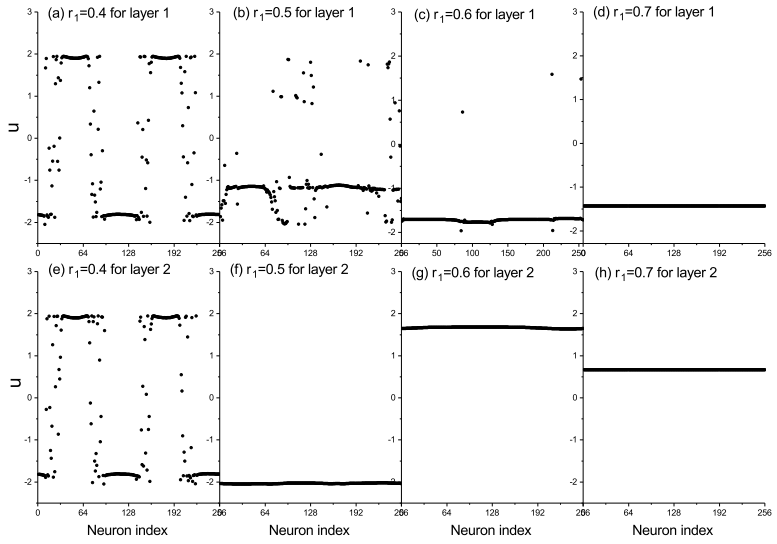

Fig. 9: Snapshots of membrane potentials of neurons in layer 1 (first row) and layer 2 (second row) at 10000ms with large feed-forward effect ($r_2 = 0.9$). (a)-(d) and (e)-(h) are under different feed-back effect strength $r_1 = 0.4, 0.5, 0.6$ and 0.7 respectively.

with small amplitude (Fig. 12(a)). At the same time, STDP coupling strength self-organize a lattice-like structure from random distribution (Fig. 12(b) and (d)). With time increasing, partially domains of disordered neuron shrink gradually and irregular neuron firings are interrupted occasionally by regular firings (Fig. 12(c)). Finally, disordered firing domains degenerate to four discontinuous points and their locations fluctuate with large amplitudes (Fig. 12(e)). Cluster forms in layer 2 at last and during its formation process, distributions of $\lambda_{i,j}$ maintain a lattice-like structure (Fig. 12(d) and (f)).

Slight increment of β induces violent changes of pattern formation. Spatial-temporal patterns with $\lambda_{i,j}$ distribution under $\beta = 0.2, 0.4$ and $\pi/2$ are provided in Fig. 13. Chimera states appear in layer 2 when $\beta > 0$ except differences in number of neurons of both of disordered and regular firing. Neurons with disordered firing as $\beta = 0.2$ is apparently more than $\beta = 0.4$ (Fig. 13(a) and (c)). Chimera states burst out of chaotic-like state relatively rapidly when β is a small positive value. Chimera state also emerges in layer 2 as $\beta = \pi/2$ and it is very similar to that of $\beta = 0.4$. But it costs a very long time to form, therefore we provide the pattern during the interval of $30000 < T < 32000$ms and neglect long process of transient formation stage (Fig. 13(e)). There corresponding $\lambda_{i,j}$ also keep to distribute in a lattice-like structure.

Scenario is different when $\beta < 0$ because there is no chimera state in layer 2. Take $\beta = -\pi/2$ for example, membrane potentials alternate between

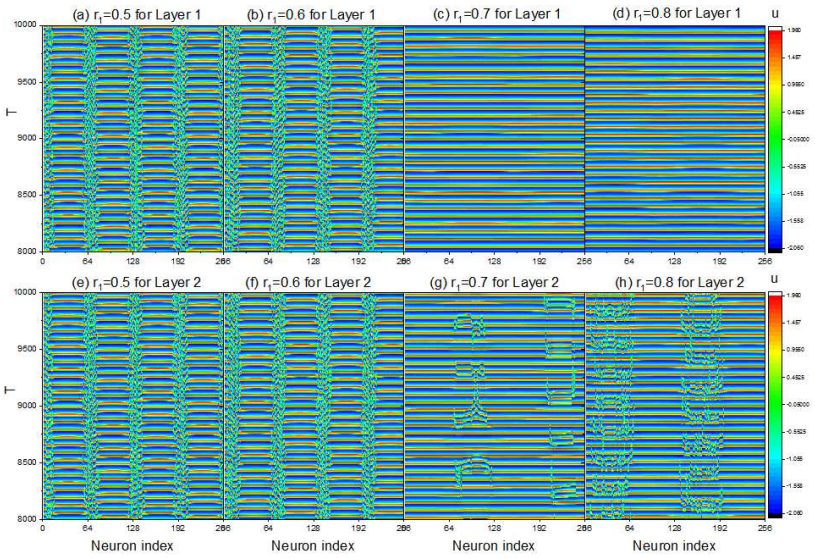

Fig. 10: Spatial-temporal patterns in layer 1 (first row) and layer 2 (second row) as 8000ms< T <10000ms with moderate feed-forward effect ($r_2 = 0.5$). (a)-(d) and (e)-(h) are under different feed-back effect strength $r_1 = 0.5, 0.6, 0.7$ and 0.8 respectively.

two values -2.1 and -1.18 at $t = 2000$ms but the mean phase velocities of all neurons are complete same (Fig. 14(a) and (b)). They fires in the same rhythm but there exist phase lags. Domains for coherent and incoherent neurons are intertwined together so that one can not distinguish them clearly in spatial-temporal pattern (Fig. 14(c)). Also, lattice-like structure of $\lambda_{i,j}$ is destroyed. The strengths of STDP coupling between incoherent neurons in chimera states of layer 1 and all neurons in layer 2 distribute around 0. The rest STDP coupling of coherent from layer 1 and all neurons in layer 2 mainly alternate between values around 0.95 and -0.47.

Finally, we employ an index based on local curvature to measure partial coherence in a network. Laplacian operator D applying on spatial date f is the key to obtain local curvature of spatial points for very snapshot, which is defied by

$$Df \equiv f(x + \Delta x, t) + f(x - \Delta x, t) - 2f(x, t) \tag{4}$$

Let D_m be the maximal absolute value of Df, which means anti-phase state between adjacent oscillators. On the contrary, spatial points whose Df approach to zero locate in synchronous region. Second we define normalized probability density function g and the fraction of synchronized regions within the whole network g_0 can be obtained by

$$g_0(t) = \int_0^{D_{th}} g(t, |Df|)\mathrm{d}|Df| \tag{5}$$

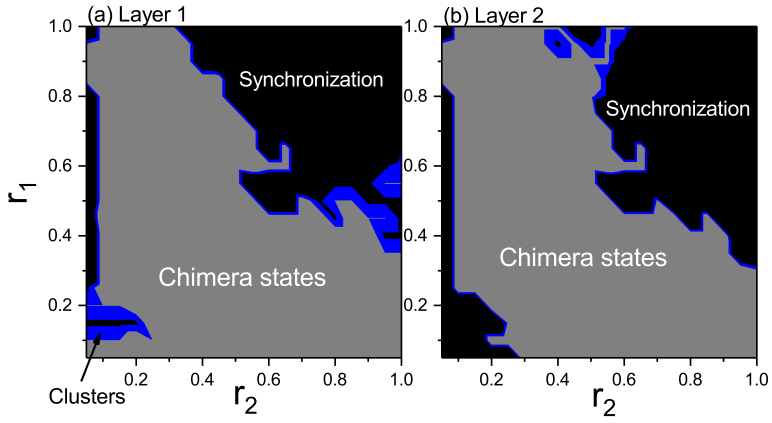

Fig. 11: Distribution of spatial-temporal patterns in parameter space of r_1 and r_2. (a) Layer 1. (b) Layer 2. Black means synchronization, Gray is chimera state, and Blue denotes cluster.

where D_{th} is the threshold value of $|Df|$ and usually chosen as $0.01 * D_m$. The time average of g_0 is denoted by $g_1 =< g_0(t) >_t$ is the index to measure the chimera state in one layer of the network. $g_1 \to 1$ means that the collective behaviors of neuron firing is in full synchronization and $g_1 \to 0$ represents complete incoherent state. g_1 in the interval $(0, 1)$ indicate the chimera state in the network.

We plot g_1 with respect to phase parameter β from $-\pi/2$ to $\pi/2$ in Fig. 15. g_1 distributes continuously around 0.2 as $\beta < 0$. Coherent neurons only occupy a small ratio of the total neuron number. Membrane potentials alternate randomly between two branches with pronounced difference. Therefore, there always exist a few adjacent neurons locate the same side of branches, which guarantee that g_1 keep in a small positive value rather than zero. g_1 rises rapidly and very close to 1 when β increase to 0, which corresponds to cluster formation. When β is greater than 0, g_1 drops a little which indicate chimera state formation. The fact that g_1 decreases gradually with small fluctuations means number of incoherent neurons within chimera state increases with respect to phase parameter of STDP.

6 Conclusions and Prospects

Feed-forward effect shows its strong ability of inducing synchronization in multi-layer network. However, neurons in collective behaviour of complete synchronization loss their capacity of coding and decoding. Chimera states as a coexistence of synchronized and disordered neurons in a network may be considered as a compromise that the multi-layer network retains part of the coding and decoding capability even under feed-forward effect. Therefore the question

paraphrased in physical language becomes that: does the chimera state exist or survive in multi-layer network modulated by feed-forward effect?

Therefore we focus on a regular multi-layer FHN neuronal network containing two layers and numerically study their patten formation . Initial condition of the first layer is chosen elaborately to guarantee emergence of chimera state and zero values are set for the layer 2. Chimera states in layer 2 emerge as the feed-forward effect strength is beyond a critical value. Under the critical value there is full synchronization as well as cluster in a narrow interval of feed-forward strength as a transient state. We also study the distribution of synchronization, cluster and chimera state in double parameters space of time-delay and strength of feed-forward effect $\tau_4 - r_2$ plane. Cluster only occupy a narrow region which separates regions for cluster and chimera state. Another type of chimera state with only two regions for disordered neuron firings is also discovered in double parameters space of time-delay of inter-layer coupling within layer 2 and strength of feed-forward effect, $\tau_4 - r_2$ plane.

Considering both feed-forward and feed-backward effect, different types of spatial-temporal patterns, including synchronization, cluster and chimera state, generate in both of layer 1 and 2 at the same time for most parameter selections. But when feed-forward effect is not very large, discrepancy on parameter selection of pattern formation for the two layers can also be observed.

Spike-timing dependent plasticity (STDP) is also introduced in feed-forward effect with small amplitude. Adaptive coupling can induce the chimera state when STDP coupling phase lag β is taken a positive value. During the chimera formation process, distribution of STDP coupling strength self-organize a lattice-like structure. Cluster with large location oscillation is discovered as $\beta = 0$. An index based on the local curvature is used to measure the pattern selection. The chimera state can survive with anti-Hebbian-like rule ($\beta \to \pi/2$) and temporally asymmetric Hebbian rule ($\beta \to 0$).

Indeed, the feed-forward effect is so strong that it can modulate the collective behaviour of neurons in multi-layer network to induce synchronization of neuron firing. Generally chimera state can only remain in the deeper layers but it need careful parameter selection. chimera states can slowly grow and encroach deeper layers in very rigorous conditions, which are small feed-forward effect and elaborately selected initial conditions. Heterogeneity, including network structure and coupling between neurons (both coupling strength and time delay) is a promising factor to break synchronization in neuronal collective behaviours and give birth to chimera state emerging in every deep layer in multiple network. It is usually believed that chimera state dominate the working principle of realistic brain network of cerebral cortex, therefore, it is urgently needed to establish a dynamical model to study parameter selection and self-adaption of network topology for chimera state in cortex.

Acknowledgements We would like to thank Prof. Changhai Tian for the very useful discussion. This work was supported by the National Natural Science Foundation of China (Grant Nos.11772242 and 11972275) and China Postdoctoral Science Foundation (Grant

No. 2018M631140), and Youth program of National Natural Science Foundation of China under Grant Nos. 12002252.

Conflict of interest

The authors declare that they have no conflict of interest.

Data availability statement

The datasets generated during and/or analysed during the current study are available from the corresponding author on reasonable request.

References

1. Hopfield J. J. Pattern recognition computation using action potential timing for stimulus representation[J]. Nature, 376(6535):33-6(1995).
2. Sheperd G. M. , The Synaptic Organization of the Brain, 5th ed. Oxford University Press, New York, (2004)
3. Bassett D. S. , Felix S. Multiscale Network Organization in the Human Brain. Multiscale Analysis and Nonlinear Dynamics. John Wiley & Sons, Ltd, (2013).
4. Richard F. B., Danielle S. B.: Multi-scale brain networks. NeuroImage 160:73-83, (2017)
5. Muldoon S. F. , Bassett D. S.: Network and Multilayer Network Approaches to Understanding Human Brain Dynamics. Philos. Sci. 83, 710 (2016)
6. Buldyrev S. V. , Parshani R. , Paul G. , Stanley H. E. , Havlin S.: Catastrophic Cascade of Failures in Interdependent Networks. Nature. 464(7291):1025 (2010).
7. elbing, D.: Globally networked risks and how to respond . Nature. 497(4774):51-59 (2013).
8. Nicosia V. , Bianconi G. , Latora V. Barthelemy M.: Growing Multiplex Networks. Physical Review Letters, , 111(5):058701 (2013)
9. Liu M. , Shao Y. , Fu X.: Complete synchronization on multi-layer center dynamical networks. Chaos Solitons & Fractals. 41(5):2584-2591 (2009)
10. Xi Y. , Wu Z. , Fu X.: Dynamical synchronization and stability of complex networks with multi-layer centers. Chaos, Solitons & Fractals, 2009, 40(2):635-641.
11. Lixin Y., Jun J., Xiaojun L.: The role of interconnection patterns on synchronizability of duplex oscillatory power network[J]. Communications in Nonlinear Science and Numerical Simulation. 93:105507. (2020)
12. Wang S. , Wang W. , Liu F.: Propagation of Firing Rate in a Feed-Forward Neuronal Network. Physical Review Letters, 96(1):018103 (2006).
13. Mormann F. , Kreuz T. , Andrzejak R. G.: Epileptic seizures are preceded by a decrease in synchronization.: Epilepsy Research, 53(3):173-185 (2003).
14. Huang, X. , Troy W. C. , Yang, Q. , Ma, H. , Laing, C. R. , Schiff, S. J. , Wu J.: Spiral Waves in Disinhibited Mammalian Neocortex. Journal of Neuroscience the Official Journal of the Society for Neuroscience. 24(44):9897-902 (2004)
15. Huang X. , Xu W. , Liang J., Takagaki K. , Wu J.: Spiral Wave Dynamics in Neocortex. Neuron, 68(5):978-990 (2010)
16. Kuramoto, Y., Battogtokh, D.: Coexistence of coherence and incoherence in nonlocally coupled phase oscillators. Nonlinear Phenom. Complex Syst. 5, 380C385 (2002)
17. Tanaka D. , Kuramoto Y.: Complex Ginzburg-Landau equation with nonlocal coupling, Phys. Rev. E 68(2), 026219 (2003)
18. Shima S. I. , Kuramoto Y.: Rotating spiral waves with phase-randomized core in nonlocally coupled oscillators, Phys. Rev. E 69(3), 036213 (2004)
19. Abrams, D. M., Strogatz, S. H.: Chimera states for coupled oscillators. Phys. Rev. Lett. 93, 174102 (2004)

20. Sethia G. C. , Sen A. , and Atay F. M.: Clustered chimera states in delay-coupled oscillator systems, Phys. Rev. Lett. 100(14), 144102 (2008)
21. C. R. Laing, The dynamics of chimera states in heterogeneous Kuramoto networks, Physica D 238(16), 1569 (2009)
22. Tian C. H. , Zhang X. Y. , Wang Z. H. , Liu Z. H.:Diversity of chimera-like patterns from a model of 2D arrays of neurons with nonlocal coupling. Front. Phys.12(3), 128904 (2017)
23. Omelchenko I. , Maistrenko Y. , Hovel P. , Scholl E.: Loss of coherence in dynamical networks: Spatial chaos and chimera states, Phys. Rev. Lett. 106(23), 234102 (2011)
24. Gu C. , St-Yves G. , Davidsen J.: Spiral wave chimeras in complex oscillatory and chaotic systems, Phys. Rev. Lett. 111(13), 134101 (2013)
25. Panaggio M. J. , Abrams D. M.: Chimera states on a flat torus, Phys. Rev. Lett. 110(9), 094102 (2013)
26. Panaggio M. J. , Abrams D. M.: Chimera states on the surface of a sphere, Phys. Rev. E 91(2), 022909 (2015)
27. Zhu, Y., Zheng, Z.G., Yang, J.Z.: Chimera states on complex networks. Phys. Rev. E 89, 022914 (2014)
28. Tang, J., Zhang, J. , Ma, J. Luo, J.: Noise and delay sustained chimera state in small world neuronal network. SCIENCE CHINA-TECHNOLOGICAL SCIENCES 062(007):1134-1140 (2019)
29. Chandran P. , Gopal R. , Chandrasekar V. K. , Athavan N.: et al. Chimera-like states induced by additional dynamic nonlocal wirings. Chaos, 30(6):063106 (2020)
30. Yao N. , Huang Z. G. , Ren H. P. , Grebogi C. , Lai Y. C.: Self-adaptation of chimera states. PHYSICAL REVIEW E 99(1) (2019)
31. Rattenborg, N.C., Amlaner, C.J., Lima, S.L.: Behavioral,neurophysiological and evolutionary perspectives on unihemispheric sleep. Neurosci. Biobehav. Rev. 24, 817C842 (2000).
32. Tamaki M , Bang J , Watanabe T , et al.: Night Watch in One Brain Hemisphere during Sleep Associated with the First-Night Effect in Humans. Current Biology Cb, 1190-1194 (2016).
33. Rothkegel A. , Lehnertz K.: Irregular macroscopic dynamics due to chimera states in small-world networks of pulse-coupled oscillators. Chaos An Interdisciplinary Journal of Nonlinear Science, 5(5):174-183 (2014)
34. Andrzejak R. G. , Rummel C. , Mormann F. , Schindler K.: All together now: Analogies between chimera state collapses and epileptic seizures. Scientific Reports. 6:23000 (2016)
35. Lainscsek C. , Rungratsameetaweemana N. , Cash S. S. , Sejnowski T.J.: Cortical chimera states predict epileptic seizures. Chaos, 29(12):121106 (2019)
36. Ghosh S , Kumar A , Zakharova A , et al. Birth and Death of Chimera: Interplay of Delay and Multiplexing. Europhysics Letters, 115(6):60005 (2016).
37. Majhi S. , Perc M. , Ghosh D.: Chimera states in uncoupled neurons induced by a multilayer structure. Scientific Reports. 6. 39033 (2016)
38. Majhi S. , Perc M. , Ghosh D.: Chimera states in a multilayer network of coupled and uncoupled neurons. Chaos,, 27(7):R67 (2017)
39. Wu Z. M. , Cheng H. Y. , Feng Y. , ; Li H.H; Dai Q.L. ; Yang, J.Z.: Chimera states in bipartite networks of FitzHughCNagumo oscillators[J]. Frontiers of Physics,, 13(2) (2017).
40. Bi, G.Q., Poo, M.M.: Synaptic modificationsinculturedhippocampal neurons: dependence on spike timing, synaptic strength, and postsynaptic cell type. J. Neurosci. 18, 10464 (1998)
41. Markram, H., Lubke, J., Frotscher, M., Sakmann, B.: Regulation of synaptic efficacy by coincidence of postsynapticaps and epsps. Science 275, 213 (1997)
42. Caporale, N., Dan, Y .: Spike timing-dependent plasticity: a hebbian learning rule. Ann. Rev. Neurosci. 31, 25 (2008)
43. Huo S. , Tian C. , Kang L. , Liu Z.: Chimera states of neuron networks with adaptive coupling. Nonlinear Dynamics, 96(1): 75-86 (2019)

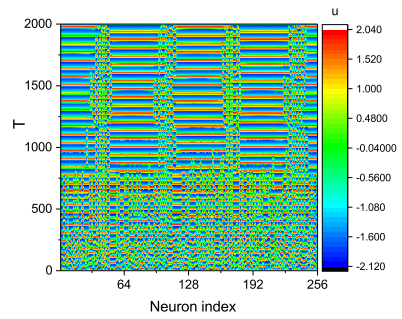

(a) Pattern during $0 < T < 2000$ms

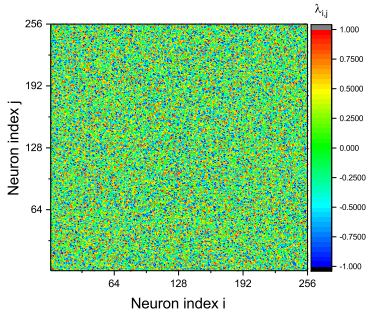

(b) $\lambda_{i,j}$ at the initial moment

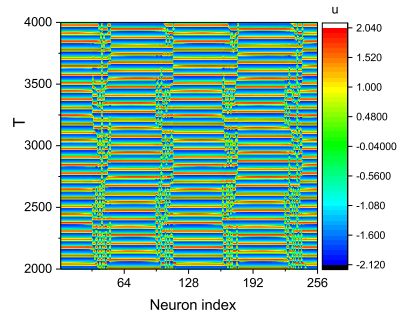

(c) Pattern during $2000 < T < 4000$ms

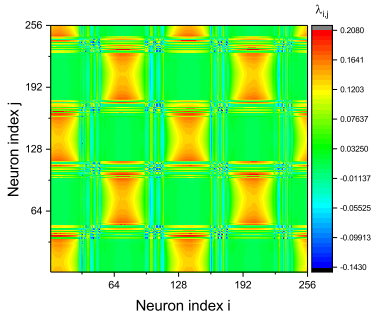

(d) $\lambda_{i,j}$ at $T = 2000$ms

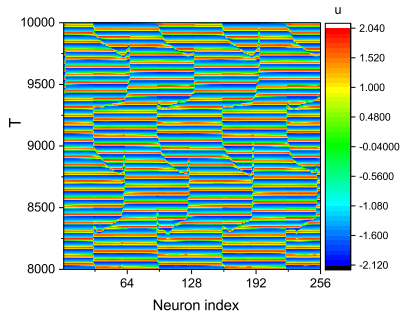

(e) Pattern during $8000 < T < 10000$ms

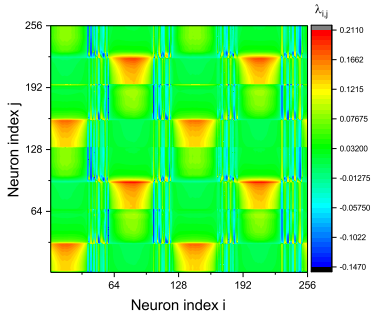

(f) $\lambda_{i,j}$ at $T = 10000$ms

Fig. 12: Spatial-temporal patterns in layer 2 (left column) at different instants and their corresponding distribution of STDP strength $\lambda_{i,j}$ (right column). (a),(c), and (e) are patterns during $0 < T < 2000$ms, $2000 < T < 4000$ms, and $8000 < T < 10000$ms respectively. (b), (d), and (f) are STDP strength across layers at 0ms, 2000ms and 10000ms respectively.

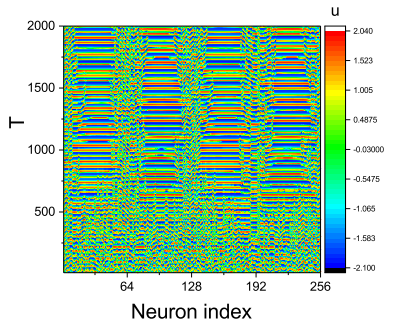

(a) Pattern as $\beta = 0.2$ during $0 < T < 2000$ms

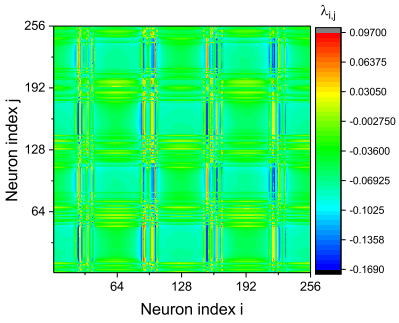

(b) $\lambda_{i,j}$ at $T = 2000$ms as $\beta = 0.2$

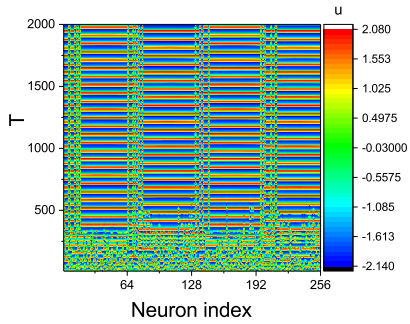

(c) Pattern as $\beta = 0.4$ during $0 < T < 2000$ms

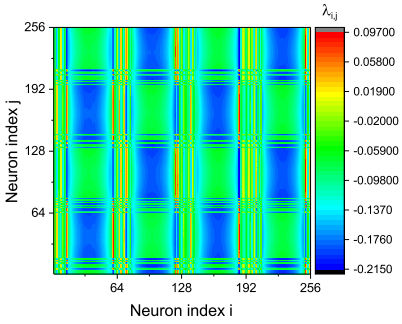

(d) $\lambda_{i,j}$ as $\beta = 0.4$ at $T = 2000$ms

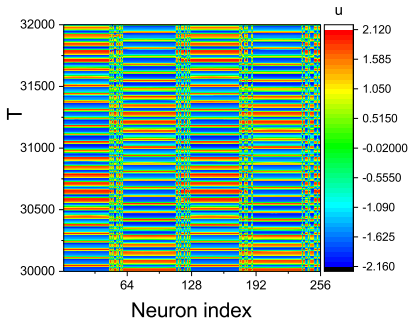

(e) Pattern as $\beta = \pi/2$ during $30000T < 32000$ms

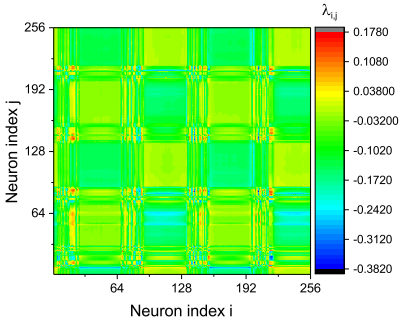

(f) $\lambda_{i,j}$ as $\beta = \pi/2$ at $T = 32000$ms

Fig. 13: Spatial-temporal patterns in layer 2 (left column) under different parameter β and their corresponding distribution of STDP strength $\lambda_{i,j}$ (right column). (a),(c), and (e) are patterns under $\beta = 0.2, 0.4$ and $\pi/2$ respectively. (b), (d), and (f) are their corresponding distributions of STDP strength across layers.

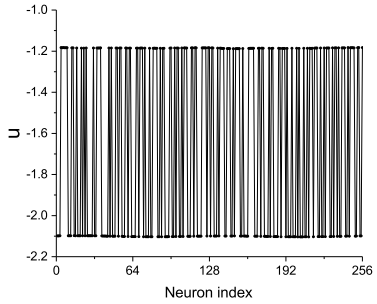

(a) Membrane potentials as $\beta = -\pi/2$ at $T = 2000$ms

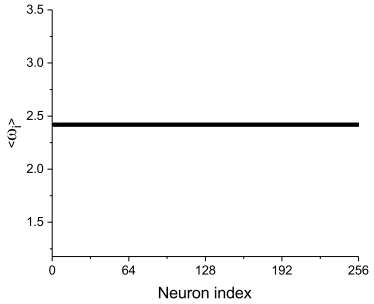

(b) $\omega_{i,2}$ as $\beta = -\pi/2$

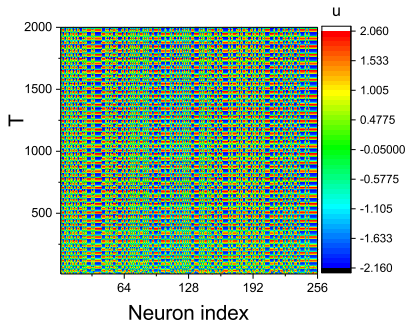

(c) Pattern as $\beta = -\pi/2$ during $0 < T < 2000$ms

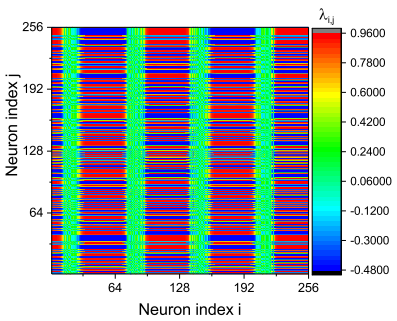

(d) $\lambda_{i,j}$ as $\beta = -\pi/2$ at $T = 2000$ms

Fig. 14: Pattern formation in layer 2 as $\beta = -\pi/2$. (a) Membrane potentials distribution at $T = 2000$ms. (b) Mean phase velocities. (c) Spatial-temporal pattern during $0 < T < 2000$ms and (c) Their corresponding distribution of STDP strength $\lambda_{i,j}$ at $T = 2000$ms.

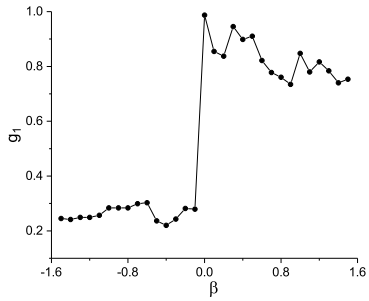

Fig. 15: Pattern coherent index g_1 respect to phase parameter β with STDP.